JOURNAL OF MAGNETIC RESONANCE 86, 445–452 (1990)

Single-Shot Diffusion Imaging at 2.0 Tesla

ROBERT TURNER

Biomedical Engineering and Instrumentation Branch, Division of Research Services, National Institutes of Health, Bethesda, Maryland 20892

AND

DENIS LE BIHAN

Diagnostic Radiology Department, Warren G. Magnuson Clinical Center, National Institutes of Health, Bethesda, Maryland 20892

Received February 27, 1989; revised July 10, 1989

A single-shot echo-planar diffusion imaging sequence (IVIM-EPI: intra-voxel incoherent motion echo-planar imaging) is presented, which is immune from the motion artifacts which may seriously impair images obtained using other diffusion imaging sequences. For a static water phantom, the measured value of diffusion constant ($D = 2.30 \times 10^{-9}$ m^2 s^{-1} at $T = 298$ K) shows excellent agreement with that obtained using a multipulse spin-echo technique and with literature values. Single-shot diffusion imaging can now be used reliably to make dynamic time-course studies with excellent time resolution.

Diffusion, like any random motion in a magnetic field gradient, results in an irreversible loss of phase coherence similar to the effect of transverse relaxation. To observe this effect it is necessary to impose gradient pulses which are either large or of long duration (*1*), and to ensure that the transverse spin magnetization is refocused, using either a 180° RF refocusing pulse or gradient reversal. The effects of molecular diffusion in NMR imaging have received attention ever since the earliest days (*2*) when it was feared that diffusion would prevent the imaging of fluid-containing objects. Fortunately, images of good resolution may be obtained using magnetic field gradients of sufficiently small magnitude that diffusion effects are normally negligible. Several methods, all utilizing diffusion gradients, have been developed for generating images with enhanced diffusion contrast, or (more generally) maps of the spatial variation of intravoxel incoherent motion (IVIM), of which we shall mention three.

The earliest method for successfully imaging IVIM used spin echoes (*3–5*). This method employed a conventional spin-warp imaging sequence with additional diffusion gradients added on either side of the refocusing 180° RF pulse, as shown in Fig. 1. The diffusion gradients are shown shaded. Images are obtained for the diffusion gradient set at zero and at a large value G_d, and images of the attenuation coefficient, $\ln(A(0)/A(G_d))$, may be displayed. This is proportional to the apparent diffusion constant, as shown in Eq. [1], below. The apparent diffusion constant may contain

0022-2364/90 $3.00

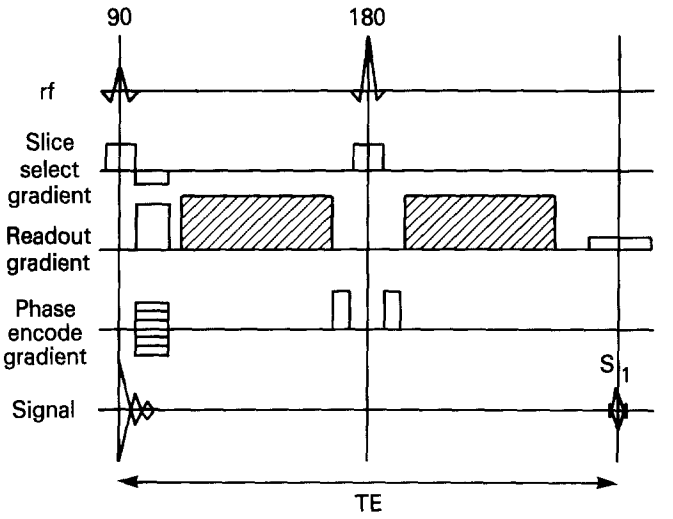

FIG. 1. Diagram of spin-echo diffusion imaging sequence IVIM-SE. Diffusion gradients are shaded. Note the crusher gradients on either side of the 180° pulse.

effects of perfusion, and the proportionality factor depends on the strength, duration, and timing of all of the applied gradients. The major disadvantage of this method is the long acquisition time of several minutes. When large or long gradients are used, motional artifact, arising from respiration, blood flow, eye motion, or even flow of cerebrospinal fluid, can be very severe.

More recently, IVIM images have been obtained using modified SSFP sequences (*6–8*), in which a large unipolar gradient is introduced between each RF pulse. If data are acquired from the echo immediately preceding each RF pulse, apparent diffusion constants may be extracted from the image data fairly easily. This method has the advantage of comparatively short imaging time, a few seconds in favorable circumstances, and thus it is less prone to motional artifact. Also worth noting is the stimulated echo sequence (*9*), which can be applied to samples for which the transverse relaxation time T_2 is very short.

What these techniques have in common is the ability to investigate regional variations of diffusion constant and perfusion in tissue quantitatively (*4, 5, 10, 11*). This opens a new window into tissue pathology and function. Temporal variations in perfusion accompany all physical activities of the body, including brain function. Diagnostically significant differences can be seen in the perfusion and diffusion characteristics of infarction, neoplasms, and other brain pathologies. PET scanning has already suggested the vast clinical and scientific potential in studying changes of cerebral blood flow during functional activity. So far, however, it has been difficult to use MRI to obtain reproducible results for changes in brain perfusion accompanying brain activity, largely because the small changes in MRI signal which might otherwise be observable are masked by large and persistent motional artifacts.

In order to minimize such artifacts, it is clearly necessary to use an imaging technique which collects all of the spatial information from the object following a single RF pulse. Such techniques are collectively known as EPI (echo-planar imaging) or

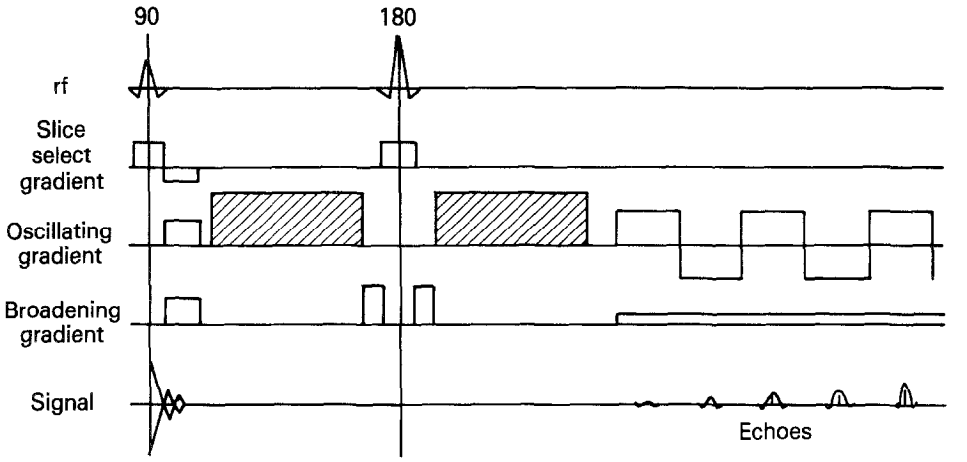

FIG. 2. Diagram of echo-planar diffusion imaging sequence IVIM-EPI. Diffusion gradients are shaded.

snapshot imaging. This paper describes the careful implementation of a modification of the standard EPI technique which includes diffusion gradients, as first suggested by Turner (*11*) and demonstrated by Avram and Crooks (*12*). This technique should thus permit the visualization of short-term variations in apparent diffusion coefficient. It is validated for a static phantom by comparison with results using a multipulse imaging sequence.

SEQUENCES

In order to increase greatly the sensitivity of the standard modulus-image echo-planar imaging sequence (*13*) to perfusion and diffusion, it is only necessary to provide a large refocused gradient for a period of time before rapid gradient switching and data acquisition (*11*). The nuclear magnetization may be refocused either by simply reversing the polarity of the gradient halfway through the period for which it is applied or by inserting a 180° RF refocusing pulse at this point, without reversing the gradient polarity. During this time diffusing spins lose some of their phase coherence, and the ensuing image is diminished in intensity. Flow which is coherent over the scale of a voxel causes no loss of signal intensity. As Avram and Crooks (*12*) have pointed out, the EPI-switched readout gradient itself, for typical amplitudes and durations used in practice, has a negligible effect on signal attenuation caused by diffusion. The phase-encode gradient, which has a small integrated magnitude, has still less effect. The sequence used is shown in Fig. 2.

A 180° RF pulse was used to refocus the magnetization, rather than a simple gradient reversal, because it was found that this method is less sensitive to hardware problems, although it requires good RF homogeneity and careful setting of the 180° pulse. Short, large amplitude, crusher gradient pulses on either side of the slice-selective 180° pulse were found to improve image quality, by removing most of the residual FID resulting from incorrect pulse setting. The crusher gradients were applied orthogonally to the diffusion gradients, and contributed less than 0.1% to the attenuation

caused by diffusion in the sample. To achieve an attenuation large enough to accurately measurable, a preparation time of 20 ms, with diffusion gradients of up to 40 mT/m, was found to be required.

Because T_2 is no more than 50–100 ms in tissue, to avoid loss of signal, it was necessary to ensure that the largest echo, nominally in the middle of the echo train, occurred no later than 50 ms after the RF pulse. The 2 T GE CSI imaging system used, fitted with 25 cm bore "Acustar" shielded gradient coils (*14–16*), was limited to a minimum intersample time of 7 μs (12 bit), and the maximum gradient available was 40 mT/m (with a rise time of 80 μs to this value). Thus, for a 64 $\times$ 64 image, the minimum total acquisition time was 28 ms, giving a spatial resolution of 2.6 mm. For the measurements reported here, the field of view was 100 mm, and the total acquisition time was 94 ms.

For comparison, 128 $\times$ 128 images of the same phantom, using the same field of view, were obtained using a diffusion-weighted spin-echo sequence (*3, 4*). The gradients and RF pulses of the two sequences prior to data acquisition were arranged to be identical, except for the defocusing lobes of the transverse gradients. For the 128 $\times$ 128 spin-echo sequence, these were required to have twice the area of those for the 64 $\times$ 64 echo-planar image, since the pixels were half the size in each direction.

DISCUSSION AND RESULTS

The relevant gradient factors, denoted as b, were calculated numerically using the formulation given by Le Bihan (*3*),

$$A(G_d) = A(0)\exp(-bD), \qquad [1]$$

where

$$b = \int_0^t |\mathbf{k}(t')|^2 dt', \qquad [2]$$

$$\mathbf{k}(t) = \gamma \int_0^t \mathbf{G}(t')dt' \qquad (t < t_0), \qquad [3]$$

$$\mathbf{k}(t) = \mathbf{k}(t_0) - \gamma \int_{t_0}^t \mathbf{G}(t')dt' \qquad (t > t_0), \qquad [4]$$

t_0 is the time at which the 180° pulse was applied, and $\mathbf{G}(t)$ is the total instantaneous magnetic field gradient, which includes the variable diffusion gradient G_d. The data were transferred by Ethernet to a Sun 3/160 workstation and analyzed using IDL (Interactive Data Language, Research Systems Inc.). The signal amplitude $A(G_d)$ was measured by selecting the same region of interest on each of a series of images acquired using different values of G_d and obtaining the mean pixel values for each image in this region. The gradient strength in each direction was previously calibrated to an accuracy of better than 1% using a phantom of precisely known dimensions. The gradient fields themselves were monitored using a flux integrator and were found to follow the DAC output with good linearity. The positions of the echoes from the EPI sequence were observed to remain stable to much better than one interacquisition interval over the entire range of diffusion gradient amplitudes, showing that the

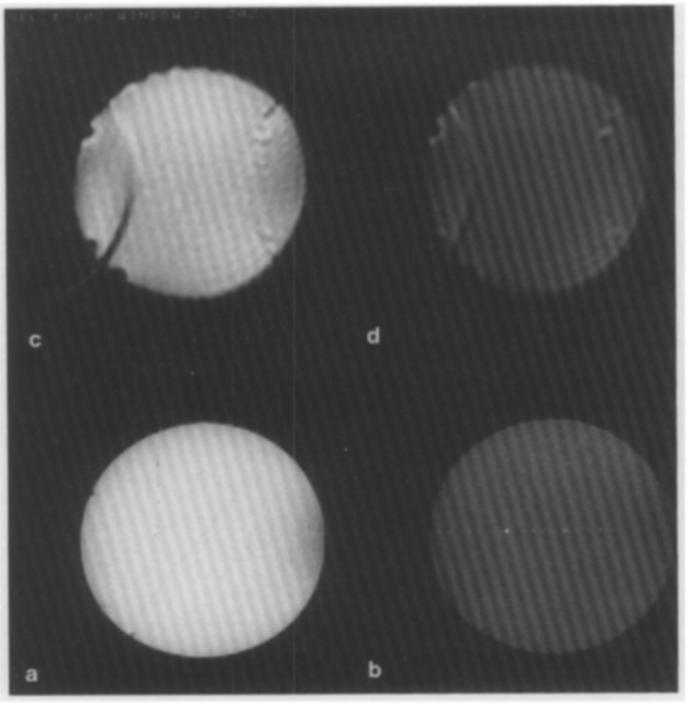

FIG. 3. Images of water phantom with varying diffusion gradients. IVIM-SE 128 × 128 images: (a) $G_d = 0$, (b) $G_d = 40$ mT m^{-1}. IVIM-EPI 64 × 64 images, Fourier-interpolated to 128 × 128: (c) $G_d = 0$, (d) $G_d = 40$ mT m^{-1}.

gradient refocusing was excellent. Progressive defocusing, arising from imperfect matching of the diffusion gradient pulses as their amplitude was increased, would in any case have caused very noticeable additional image artifacts.

Figure 3 shows typical source images for two values of G_d of a copper-sulfate-doped water phantom, from the echo-planar sequence IVIM-EPI, and from the spin-echo sequence IVIM-SE. There is a noticeable ghost on the EPI images; this is a result of a serious hardware limitation of our machine, which makes it very difficult to allow the ADC sampling time to vary over the course of data acquisition. Thus data are continuously acquired even during the appreciable fraction of the time when the gradient is being switched from one polarity to the other. The oscillating gradient waveform is characteristically slightly asymmetrical in time, being more rounded on the leading edge than on the trailing edge, over a time of about 50 μs. This has a number of causes, including small residual eddy currents associated with the rapid switching of the gradient. Thus some data points are acquired at unequal intervals in k space, and each echo is not precisely symmetrical. A detailed phase correction for this effect is theoretically possible, but cannot be implemented on-line using CSI software. Since alternate echoes in the data set must be time-reversed during image reconstruction, the time-reversal asymmetry in the gradient waveform gives rise to a double-period variation in the processed data, and hence to the 180° ghost apparent in these images. The region of interest selected for purposes of comparison with IVIM-

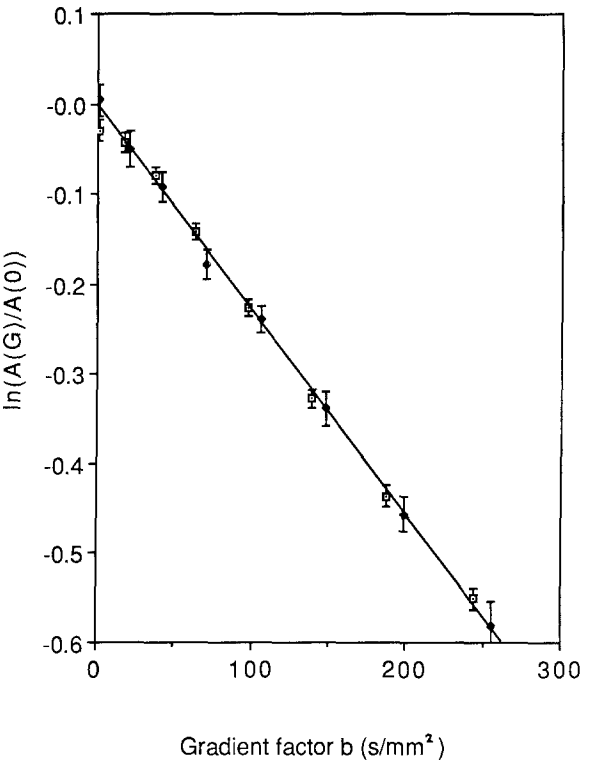

FIG. 4. Dependence of normalized mean image pixel intensity of images of a water phantom on gradient factor b. Diamonds and linear fit: IVIM-SE results. Open squares: IVIM-EPI results.

SE images, and calculation of the diffusion constant, did not include that part of the image on which the ghost encroached. The single-shot signal:noise ratio of the IVIM-EPI images was approximately 60:1 for $G_d = 0$.

Figure 4 presents a comparison between the normalized image amplitudes obtained as described earlier from the IVIM-SE sequence and the IVIM-EPI sequence, plotted against the appropriate gradient factor b, calculated carefully using Eqs. [2]–[4]. The error bars represent the variations in pixel value over the regions of interest selected, and the smaller error bars for the echo-planar results reflect the use of a somewhat larger region of interest. There is a small difference between the b factors for a given value of G_d, arising from the difference in dephasing gradients noted previously. A cross term, involving the dephasing gradient and G_d, enters when b is calculated correctly according to Eqs. [1]–[4], which cannot be neglected if precise determination of the diffusion constant is required. This cross term arises from the fact that the spins are already defocused by the initial lobe of the read gradient, before the diffusion gradient itself is applied in the same direction, which gives an *added* dephasing. Since it is the *square* of the total dephasing which enters into the attenuation due to diffusion, the cross term appears.

The agreement of the two data sets is highly satisfactory, except at small diffusion gradients, for which the EPI image amplitudes were somewhat lower than those of

the SE images. Examination of the raw data showed that some slight, interfering, contamination of the EPI echo train by the small residual FID following the 180° pulse was responsible for this. Larger diffusion gradients crushed this FID altogether.

The data shown in Fig. 4 were fitted to Eq. [1] using the standard Marquardt nonlinear least-squares fitting algorithm, giving the mean diffusion constant within the region of interest. We found, at $T = 298$ K, $D = 2.30 \pm 0.07 \times 10^{-9}$ m^2 s^{-1} (evaluated from all eight IVIM-SE data points), and $D = 2.30 \pm 0.06 \times 10^{-9}$ m^2 s^{-1} (from the final seven IVIM-EPI data points). These values are in excellent agreement with each other and with literature values for the diffusion constant of water (*17*), although somewhat lower than those obtained by Avram and Crooks (*12*). These workers, using the formulation of Stejskal and Tanner (*1*), neglected to include the effect of the defocusing lobe of the transverse imaging gradient in the same direction as the diffusion gradient on the b factor of Eq. [2] and hence underestimated the magnitude of b.

In order to confirm the technique's insensitivity to bulk motion of the object, a more structured phantom was moved by a few millimeters between successive image acquisitions, with and without a large applied diffusion gradient. The diffusion image was then calculated, and the expected simple misregistration artifact was observed in regions of abrupt change in pixel intensity, such as edges. Where the image and phantom were uniform, the diffusion constant was measured to be the same, whether or not the phantom was moved between acquisitions.

CONCLUSIONS AND IMPLICATIONS

It is clear that reliable values of the diffusion constant of fluids can be obtained using a single-shot imaging technique. In principle only two images need be acquired in order to compute a map of the diffusion constant. For sequential time-course studies *in vivo* a control image, with zero diffusion gradient, can be obtained first, and used to normalize subsequent diffusion-weighted images, thus providing qualitative maps of rapid changes in diffusion and perfusion. The time resolution for observing such changes, assuming that the signal:noise ratio was adequate for single-shot determination of the apparent diffusion constant, could be as short as one second. Motion artifact is obviously not a problem: misregistration of the diffusion-weighted and control images caused at worst an easily interpreted blurring of the diffusion image, rather than the highly deceptive artifact distributed over the entire image often found using multipulse image acquisition techniques.

The EPI images presented here have 64×64 resolution. A recent software upgrade of the CSI system used has now allowed 128×128 images to be obtained, although with a minimum acquisition time of 114 ms. For organs with a relatively long T_2, such as the brain, it will soon be possible to obtain single-shot diffusion images of animal models at this resolution.

ACKNOWLEDGMENTS

We thank the NIH In Vivo NMR Center for provision of its excellent facilities and support, and Peter van Zijl and Chrit Moonen for their advice and assistance. The EPI sequence was implemented on the GE CSI machine with the help of Christopher Sotak. We are most grateful to James Pekar, who wrote the

image analysis software, and to the anonymous referee who suggested the experiment to verify motion artifact insensitivity.

REFERENCES

1. E. O. STEJSKAL AND J. E. TANNER, *J. Chem. Phys.* **42,** 288 (1964).
2. P. MANSFIELD, *J. Phys. C* **6,** L422 (1973).
3. D. LE BIHAN, E. BRETON, AND A. SYROTA, *C. R. Acad. Sci.* **301,** 1109 (1985).
4. D. G. TAYLOR AND M. C. BUSHELL, *Phys. Med. Biol.* **30,** 345 (1985).
5. D. LE BIHAN, E. BRETON, D. LALLEMAND, E. CABANIS, AND M. LAVAL-JEANTET, *Radiology* **161,** 401 (1986).
6. D. LE BIHAN, *Magn. Reson. Med.* **7,** 346 (1988).
7. D. LE BIHAN, R. TURNER, AND J. MCFALL, *Magn. Reson. Med.* **10,** 324 (1989).
8. K. D. MERBOLDT, M. L. GYNGELL, W. HAENICKE, J. FRAHM, AND H. BRUHN, "Proceedings, 7th Annual Meeting SMRM, San Francisco," p. 604, 1988.
9. K. D. MERBOLDT, W. HAENICKE AND J. FRAHM, *J. Magn. Reson.* **64,** 479 (1985).
10. D. LE BIHAN, E. BRETON, D. LALLEMAND, M. L. AUBIN, J. VIGNAUD, AND M. LAVAL-JEANTET, *Radiology* **168,** 497 (1988).
11. R. TURNER, *in* "Cerebral Blood Flow" (A. Rescigno and A. Boicelli, Eds.), p. 245, Plenum Press, New York, 1988.
12. H. E. AVRAM AND L. E. CROOKS, "Proceedings, 7th Annual Meeting SMRM, San Francisco," p. 980, 1988.
13. A. H. HOWSEMAN, M. K. STEHLING, B. CHAPMAN, R. COXON, R. TURNER, R. J. ORDIDGE, M. G. CAWLEY, P. GLOVER, P. MANSFIELD, AND R. E. COUPLAND, *Brit. J. Radiol.* **61,** 822 (1988).
14. P. MANSFIELD AND B. CHAPMAN, *J. Magn. Reson.* **66,** 573 (1986).
15. R. TURNER AND R. M. BOWLEY, *J. Phys. E* **19,** 876 (1986).
16. P. B. ROEMER, W. A. EDELSTEIN, AND J. S. HICKEY, "Proceedings, 5th Annual Meeting SMRM, Montreal," p. 1067, 1986.
17. R. MILLS, *J. Phys. Chem.* **77,** 685 (1973).